Indian Journal of Chemical Technology
Vol. 30, November 2023, pp. 832-839
DOI: 10.56042/ijct.v30i6.6548

Catalytic activities of green synthesized silver, gold and bimetallic (Ag-Au) nanoparticles

Ramanjeet Kaur[1], Pramod K Avti[2]*, Vivek Kumar[3] & Rajesh Kumar[1]*
[1]Department of Physics, Panjab University Chandigarh-160 014, India
[2]Department of Biophysics, Post Graduate Institute of Medical Education and Research, Chandigarh-160 012, India
[3]Centre for Medical Physics, Panjab University, Chandigarh-160014, India
*E-mail: rajeshphysicspu@gmail.com

Received 9 September 2022; accepted 07 August 2023

Bimetallic (Ag-Au/ Au-Ag) nanoparticles have been synthesized using *Litchi chinesis* leaf extract and characterised using UV-visible spectroscopy, dynamic light scattering (DLS), zeta potential and transmission electron microscopy (TEM). The hydrodynamic size of Ag-Au/Au-Ag NPs are found to be 83 nm/ 90 nm, respectively, by DLS techinque. The catalytic capability of green synthesised silver, gold and bimetallic(Ag-Au) nanoparticles is described in this study by choosing the degradation of methylene blue, as a model dye.

Keywords: Ag-Au NPs, Au-Ag NPs, Bimetallic, catalytic activity, Green synthesis, Methylene blue degradation

Nanoscience and technology encompass a broad range of research and development activities that has exploded in popularity throughout the world in recent years. Nanomaterials are becoming increasingly important as a result of their numerous uses in industries such as healthcare[1], cosmetics[2], food[3], biomedical sciences[4], medication and gene delivery, diagnosis[5], catalytic[6], and cancer therapy[7]. New physico-chemical features of noble metal nanoparticles have been discovered, which are not seen in individual molecules or bulk metals. Silver and gold nanoparticles are particularly important because of their wide range of applications in sectors such as catalysis, pharmaceuticals, and sensing technology. Bimetallic nanoparticles are made up of two different metals and typically take the form of alloy nanoparticles, core-shell nanoparticles, or clusters inside clusters. They possess exceptional electrical, chemical, and catalytic qualities. Changing the components often impacts their important physical and chemical performances as well as their morphologies. The size, shape, composition, and metal distribution of bimetallic nanoparticles all have an impact on the colour that may be seen in colloidal dispersions. The peak noticed for core-shell structures depends on the metal present at the surface of particle whereas for alloyed structures, the peak of the solution is largely determined by the metal present in excess[8]. The localised surface plasmon resonance (SPR), an optical phenomena of light interacting with conducting nanoparticles, is the source of the optical features in noble metal nanoparticles. The form, size, and dielectric characteristics of nanoparticles strongly influence the position of SPR's strong resonance absorbance peak in the visible light spectrum[9].

Conventional procedures for synthesis of nanoparticles have proven to be difficult since they are expensive, time-consuming, use high dose of chemicals and solvents, and produce dangerous byproducts and limited yields. Researchers are attempting to replace these synthesizing techniques of nanoparticles with non-toxic, clean, and eco-friendly green chemistry methods due to environmental concerns. The use of plant extracts for nanoparticle production is considered a green technology since it is a simple, efficient, low-cost, and safe method.

Many studies on the production of nanoparticles employing plant extracts as both reducing and stabilising agents have been published[10,11]. In this report, the litchi leaf extract was utilized for the preparation of Ag–Au core shell nano particles (NPs). The major compounds of *Litchi chinensis* are: alkaloids, flavonoids, epicatechin ($C_{15}H_{14}O_6$), procyanidin A2 ($C_{30}H_{24}O_{12}$), proanthocyanidin B2 ($C_{30}H_{26}O_{12}$), terpenoids and steroids. The reducing and scavenging power of epicatechin is more than that of procyanidin A2, proanthocyanidin B2.

The inappropriate water waste treatment of textile industries has resulted in the discharge of several

hazardous dyes into water sources. Methylene blue (MB) dye is hazardous to the environment. The catalytic activity of green synthesized silver, gold and bimetallic (Ag-Au/Au-Ag) nanoparticles in the degradation of the colourants MB using the reducing agent $NaBH_4$ are described in this paper.

Experimental Section

Material and chemicals

Silver nitrate ($AgNO_3$), trisodium citrate ($Na_3C_6H_5O_7$), polyvinyl pyrrolidone $(C_6H_9NO)_n$, sodium borohydride ($NaBH_4$), hydrochloroauric acid ($HAuCl_4.3H_2O$) were obtained fron Sigma Aldrich and methylene blue ($C_{16}H_{18}ClN_3S$) was obtained from Loba Chemie Pvt. Ltd. (Mumbai, INDIA). Fresh leaves of *Litchi chinensis* leaves were collected from the botanical garden of the University.

Preparation of Litchi chinensis leaf extract

Litchi chinensis leaves were washed with tap water and then with deionised water to remove dust and dirt particles. Then leaves were dried and powdered finely using a grinder. 3 g of leaf powder was boiled in 50 mL of DI water for 20 min. The leaf extract was filtered through Whatman filter paper No. 1 and stored at 4°C for further use.

Synthesis of bimetallic nanoparticles

Synthesis of AgNPs and AuNPs

AgNPs and AuNPs were synthesized using *Litchi Chinensis* leaf extract, reported method[12]. $AgNO_3$ (1 mM) $HAuCl_4.3H_2O$ (1 mM) was kept on a magnetic stirrer. After that 15 µL of the prepared LCLE solution was added drop wise to $AgNO_3$ (1 mM) and $HAuCl_4.3H_2O$ (1 mM) solution. The colour of the solution changes to dark brown and red wine within a few minutes, which indicates the formation of Ag-NPs and Au-NPs, respectively.

Synthesis of bimetallic nanoparticles

The same synthesis procedures for the reduction of metallic salt as are utilised for pure metallic NPs were employed to cover the surface of the generated metallic nanoparticles, which were serving as a seed, with another metal as a shell. The nanoparticles prepared in above section were used for further bimetallic synthesis of silver coated gold nanoparticles (Au-Ag NPs) and gold coated silver nanoparticles (Ag-Au NPs). Gold coating on AgNPs and silver coating on AuNPs, we prepared fresh solution of $HAuCl_4.3H_2O$ (1 mM) and $AgNO_3$ (1 mM), we add AgNPs and AuNPs to freshly prepared solution of $HAuCl_4.3H_2O$ (1 mM) and $AgNO_3$ (1 mM), respectively with vigorously stirring on magnetic stirrer. The colour of the solution changes to blue and brick red which indicates the formation of bimetallic Ag-Au NPs and Au-Ag NPs respectively[13].

Characterization of bimetallic nanoparticles

UV–visible spectral experiments were performed using the LABINDIA UV-3000$^+$ spectrometer, to record surface plasmon resonance (SPR). It was used to obtain absorption spectra of bimetallic nanoparticles and dye degradation at various intervals of time. The development of spherical Bimetallic (Ag-Au) NPs is indicated by SPR peak at 551 nm. Transmission electron microscope (Hitachi H-7500, Japan) operating at voltage of 120 kV and equipped with CCD camera is used for the ultrastructural determination of synthesized bimetallic NPs. This instrument has the high resolution of 0.36 nm with 40–120 kV operating voltage and can magnify object up to 0.6 million times in high resolution mode. The particle shape and size were analyzed by TEM. The size distribution and surface charge value of bimetallic NPs was carried out using Malvern zetasizer (ZEN3600).

Catalytic degradation assay

The following procedure was used to catalyse the decay of the coloured methylene blue (MB) to colourless. The experiment was carried out with 0.5 mL dye (1 mM) solution, 1 mL freshly prepared $NaBH_4$ (0.1 M) solution, and manufactured AgNPs (0.05 mL) /AuNPs (0.05 mL)/ Ag-Au NPs (0.05 mL). The complete dye degradation process was carried out at room temperature without adding any pH modifying agent. The control experiment was also carried out without addittion of nanoparticles. The reaction kinetics were investigated by studying variations in the absorbance of the peak at 664 nm as the concentration of methylene blue changed over time. Degradation spectra in the region of 300–700 nm were collected. The percentage of degradation in each of the reaction was calculated using the following equation (1)

$$Decoloration\ \% = \frac{(C_0 - C_t)}{C_0} \times 100\% \qquad \ldots.(1)$$

Where C_0 and C_t are the concentration of dye at intial time 0 and at any time t.

Result and Discussion

Characterisation

Fig. 1 represents the UV-visible absorbance behaviour of monometallic (Ag-NPs/Au-NPs) and

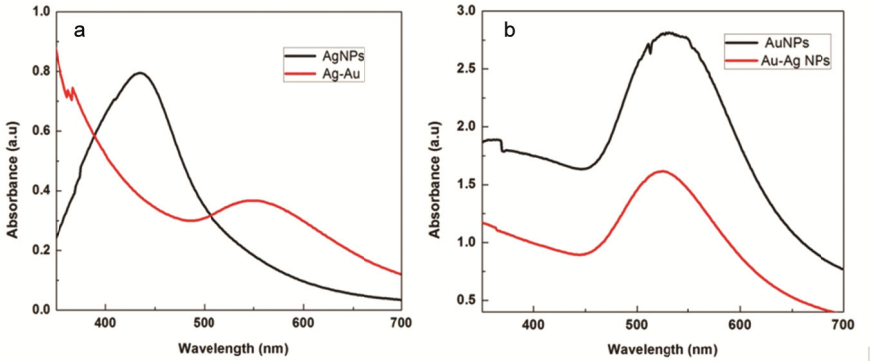

Fig. 1 — SPR spectra of synthesised NPs

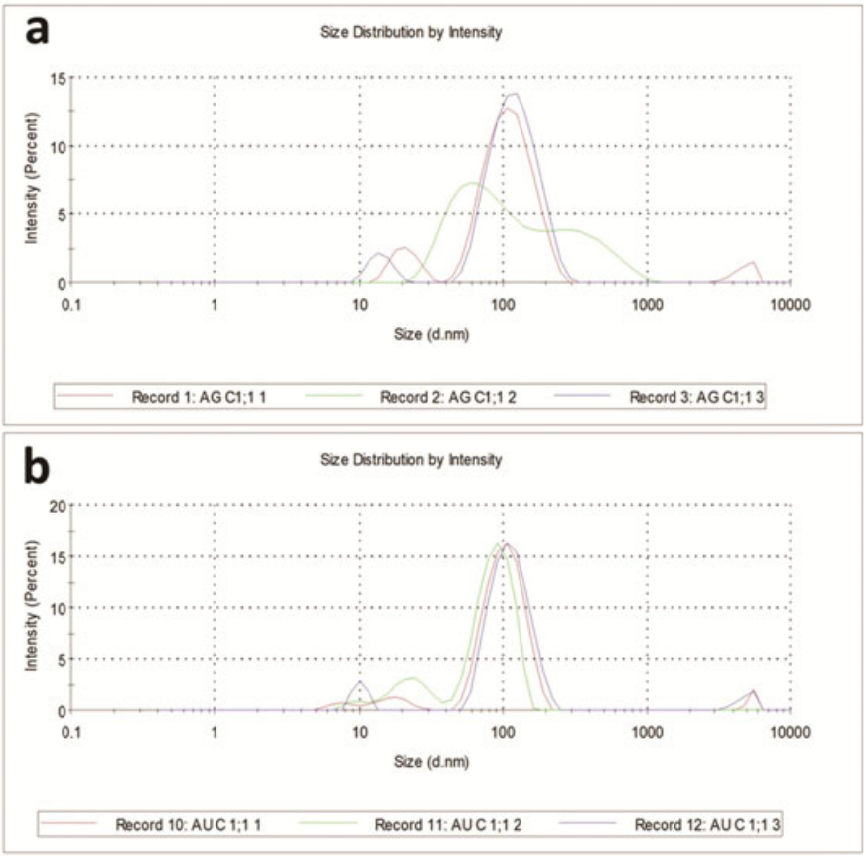

Fig. 2 — DLS of bimetallic (a) (Ag-Au) NPs and (b) (Au-Ag) NPs

bimetallic (Ag-Au/Au-Ag) nanoparticles as well as their individual and physical mixtures. The Ag-NPs and Au-NPs had a distinctive surface plasmon resonance (SPR) peak centred at 436 nm and 536 nm, but the bimetallic NPs lacked this peak. In contrast to the physical mixing sample, the Au-NPs/ Ag-NPs SPR band was not present in the bimetallic NPs sample. The production of Ag-Au/Au-Ag NPs bimetallic clusters rather than phase-separate monometallic NPs is evidently suggested by these data. SPR of Ag-NPs, Ag-Au NPs, Au-NPs and Au-Ag NPs at 436 nm, 551 nm, 536 nm and 529 nm, respectively. The gold coating over the Ag-NPs exhibits red shift from 436 nm to 551 nm and silver coating over Au-NPs exhibits blue shift from 536 nm to 529 nm[14]. The Fig. 1 clearly indicates the shift in SPR.

Fig. 2 shows graphical distribution of size of Ag-Au/Au-Ag NPs in range 40 nm - 110 nm. The average hydrodynamic size of Ag-Au NPs and Au-Ag NPs were found to be 83 nm and 90 nm, respectively. Zeta potential is a crucial factor that influences the stability

of collidal dispersion since it measures the strength of the electrostatics replusion between charged nanoparticles. Collidal nanoparticles having high the zeta potential show less aggregation, and high stability. The surface charge of the particles is determined by their zeta potential, which is depicted in Fig. 3 at -26.0 mV, -20.6 mV, -13.5 mV and -18.8 mV for Ag-Au NPs, Au-Ag NPs, Ag-NPs and Au-NPs, respectively. The high negative charge on Ag-Au/ Au-Ag NPs is a sign of stability of the nanoparticles after being synthesized. The feasibility of negative charge on bimetallic nanoparticles could be due to the capping agent of leaf extract componets[12].

Fig. 4 shows the TEM micrographs of Ag-Au NPs. TEM images reveals that most of nanoparticles were spherical in shape. The size of synthesized nanoparticles were in range of 8 nm – 50 nm and their average particles size was found to be 23 nm.

Catalytic activity

The removal of dyes is a significant problem since 10–20% of them are lost in wastewater streams[15,16]. The easiest technique to lessen the poisonous effects of these dyes is to use $NaBH_4$ as a reductant to change them into less hazardous compounds. In order to create additional non-toxic goods, these products are alternatively lowered. The reduction of dyes by BH_4^{-1} ions is kinetically unfavourable, though, and such reactions move slowly without a catalyst. This might be as a result of the energy barrier between BH_4^{-1} ions and substrate dyes[17]. Non-catalytic dye reduction takes longer time. Metal NPs exhibits excellent catalytic activity for dye reduction and have a wide surface area for reactant adsorption. Metal NPs really offer a new route for the reactants with a low level energy barrier and quickly convert them into products[17]. As a result, metal NPs catalysts serve as conveyor

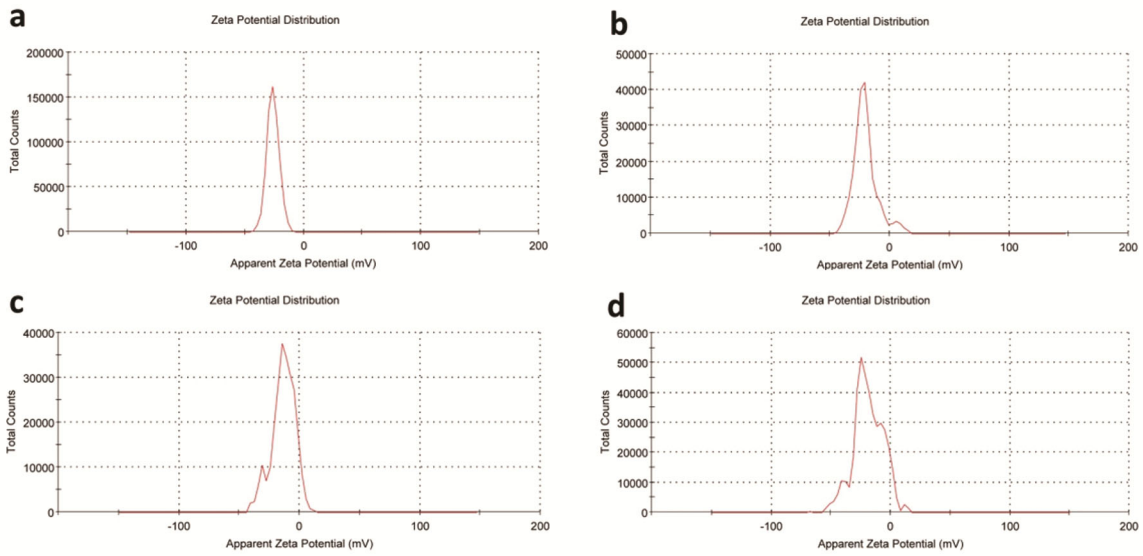

Fig. 3 — Zeta Potenial of Bimetallic (a) Ag-Au NPs (b) Au-Ag NPs, (c) AgNPs and (d) AuNPs

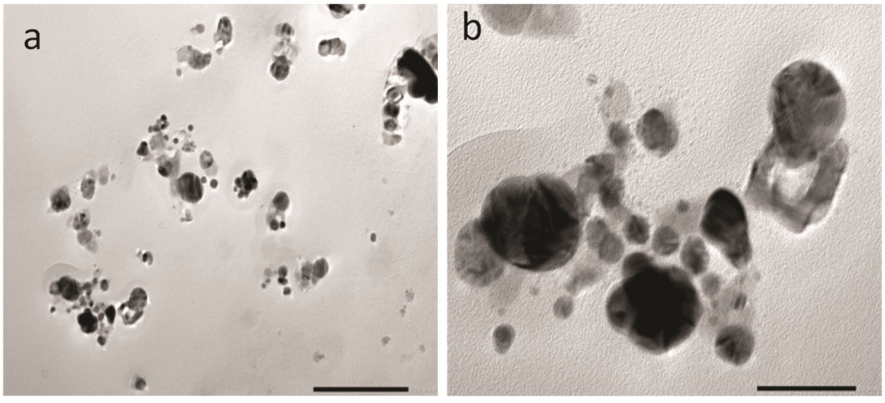

Fig. 4 — TEM images of Ag-Au NPs

belts for the passage of electrons from reductant to substrate and promote the reduction of harmful dyes.

The catalytic activity of green synthesized AgNPs/ AuNPs/ Ag-Au/ Au-Ag NPs for the degradation of MB was investigated along with the reducing agent $NaBH_4$. The absorption maxima of MB dye did not overlap with the SPR band of silver/gold/bimetallic nanoparticles, making them appropriate for catalytic research. When MB is in oxidation form, it is blue, but when it is reduced, it becomes colourless leucomethylene blue. Fig. 5 shows the absorption spectra of MB reduction by $NaBH_4$ in the absence of the synthesised catalyst. In the aqueous phase, sodium borohydride alone is incapable of reducing MB, which has a maximum wavelength of 664 nm. The degradation of the dye was catalysed by the synthesised NPs, as evidenced by the decolourization of the reaction contents. UV-visible absorption spectroscopy was used to monitor the degradation response in real time. In aqueous solution, MB generally exhibits an absorption maximum band about 664 nm due to the $\pi \rightarrow \pi^*$and $n \rightarrow \pi^*$transitions[18].

Fig. 5(a) and 5(b) shows the absorbance intensity of MB dye alone and absorbance intensity was 2.464. On the addition of $NaBH_4$ there was no reduction in absorbance intensity. The addition of Ag-NPs or Au-NPs in mixture of MB and $NaBH_4$ leads to decrease in the absorbance intensity darsically. The catalyst serves as a carrier for the hydride and electron transfer from borohydride to dye and the dye degration process become faster. The MB dye degrade upto 95.15% and 82% within 20 min and 8 min, for Ag-NPs and Au-NPs as catalyst, respectively. Similarly for the bimetallic nanoparticles act as catays ts degradation of dye shown in Fig. 5(c) and (d). The absorbance intensity decreases on addition of Ag-Au/Au-Ag NPs in mixture of MB and $NaBH_4$. MB reduced to colourless solution within 5 min and 10 min for Ag-Au NPs and Au-Ag NPs, respectively.

The %degradation of MB was calculated using Eq. (1). The findings show that Ag-Au NPs had the maximum catalytic activity (98.13%) for MB degradation after 5 min in the presence of $NaBH_4$. When compared to Au-NPs (82%), Ag-NPs (95.17%)

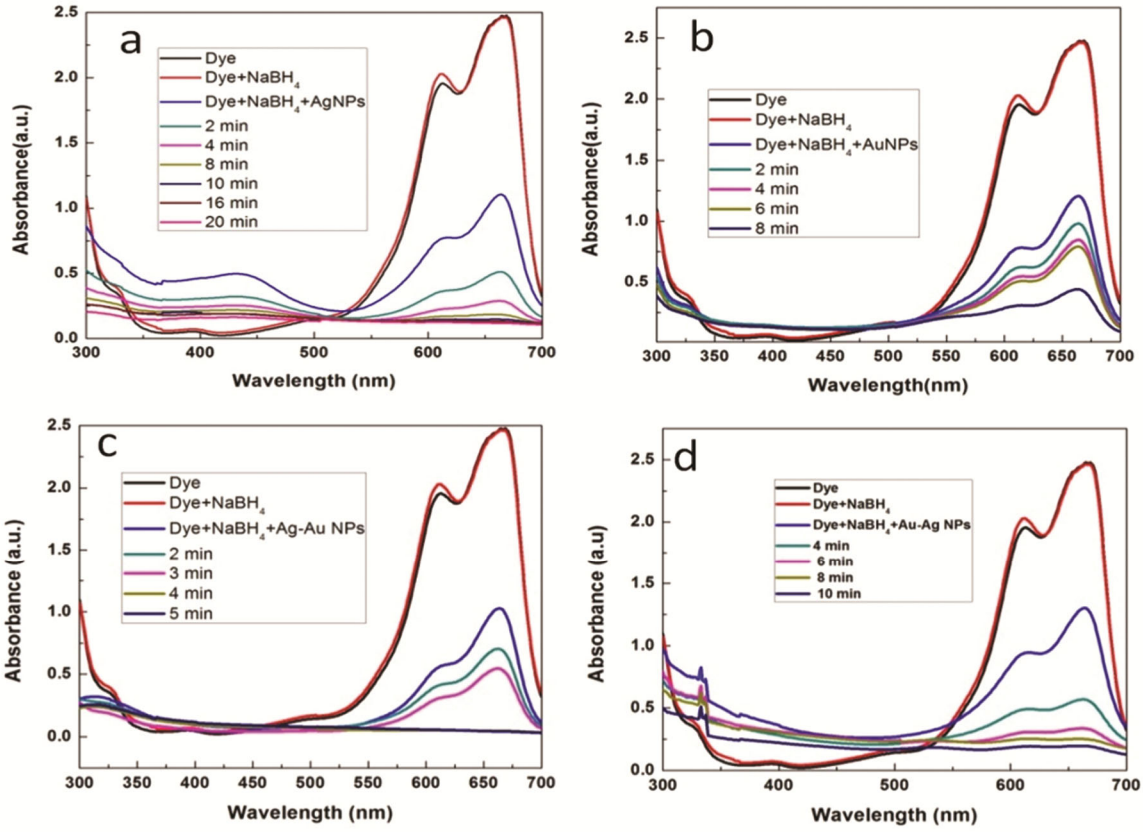

Fig. 5 — UV- Vis absorbance spectra of (a) AgNPs+MB+$NaBH_4$, (b) AuNPs+MB+$NaBH_4$ (c) Ag- Au NPs+MB+$NaBH_4$ and (d) Au- Ag NPs+MB+$NaBH_4$

and Au-Ag NPs (92.04%), the dye degradation performance of Ag-Au NPs as a catalyst was substantially superior as shown in Fig. 6.

The rate of degradation is a crucial indicator of the degradation processes. The dye degradation rate at a particular time interval is determined by how far the dye degradates from the initial concentration. By fitting the experimental data to pseudo first order and second order models, the degradation kinetics of MB over metal nanoparticles were understood. The Eq. (2) below represents the first order kinetic[19]

$$\text{In}\,(q_e - q_t) = \text{In}\,(q_e) + k_1 t \qquad (2)$$

Where q_e is the amount of dye degradated at equilliurium, q_t is the amount of dye degradated at any time t and k_1 is pseudo first order rate contant. The regression coefficient was less than 0.90 when the model was fitted to the experimental data, and there was only a moderate connection. As a result, it can be stated that the degradation process does not follow pseudo first order kinetics, and the likelihood of pseudo first order kinetics has been eliminated. The data was further put to the test using pseudo second order rate kinetics. The Eq. (3) for pseudo second order kinetics is given below [20]

$$\frac{t}{q_t} = \frac{1}{k_2 q_e^2} + \frac{t}{q_e} \qquad (3)$$

Where k_2 represents the second order rate constant. The pseudo second order kinetic model fits well, according to the current finding. As a result, the pseudo-second-order model can accurately represent the degradation behaviour of metal NPs for MB. The rate constant observed from pseudo second order kinetics was 1.05 min^{-1}, 0.732 min^{-1}, 0.5922 min^{-1} and 0.113 min^{-1} of Ag-Au NPs , Au-NPs, Au-Ag NPs and Ag-NPs, respectively. Higher the rate constant lesser the time to degrade the dye. Ag-Au NPs have higher rate constant and hence faster degradation as compared to Ag-NPs, Au-NPs and Au-Ag NPs.

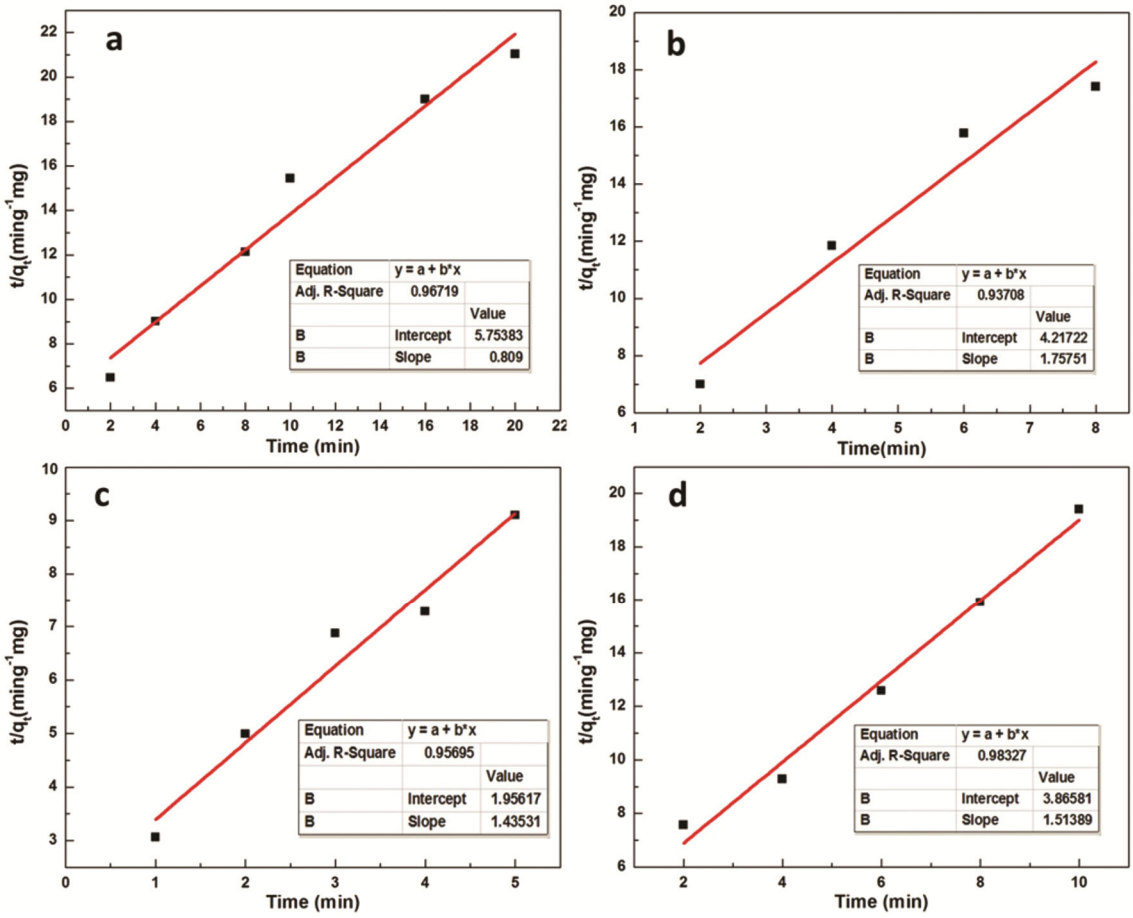

Fig. 6 — The Linear fitting of pseudo second order (a) AgNPs+MB+$NaBH_4$, (b) AuNPs+MB+$NaBH_4$ (c) Ag- Au NPs+MB+$NaBH_4$ and (d) Au- Ag NPs+MB+$NaBH_4$

Table 1 — The comparative results report with already reported methods

Catalysts	Reagent	% of degradation	Time (min)	% degradation per unit time	References
Au-Ag NPs	$NaBH_4$	94.48	5	18.89	[25]
AgNPs	$NaBH_4$	52.93±0.28	5	10.58	[25]
AuNPs	$NaBH_4$	96.93±0.21	5	19.38	[25]
AuNPs	$NaBH_4$	100	12	8.33	[26]
AuNPs	$NaBH_4$	49.62	60	0.82	[27]
AuNPs	$NaBH_4$	75.35	240	0.31	[28]
AuNPs	$NaBH_4$	94.81	4	23.70	[29]
AgNPs	-	85	315	0.26	[30]
AuNPs	-	42	330	0.12	[30]
AgNPs	$NaBH_4$	95.17	20	4.75	Present work
AuNPs	$NaBH_4$	82	8	10.25	Present work
Ag-AuNPs	$NaBH_4$	98.13	5	19.62	Present work
Au-Ag NPs	$NaBH_4$	92.04	10	9.20	Present work

The degradation of dye is a secondary step, because the dye can be degraded only when it is transferred over the catalysts surface. Since the used dye is cationic in nature, the primary mechanism of MB adsorption on the surface of metal nanoparticles is electrostatic attraction, and the increased mass transfer capacity over metal NPs may be caused by their higher negative charge[21]. Ag-Au NPs have higher zeta potential value as compare to Ag-NPs, Au-NPs and Au-Ag NPs. So, higher negative surface, cause higher mass transfer over the metal surface which is also a factor to degrade the MB in lesser time and more efficiently[22]. The bond dissociation energy is a significant factor in the breaking and/or production of new bonds during chemical reactions. The interaction between MB dye and $NaBH_4$, in which $NaBH_4$ acts as a donor and the dye as an acceptor, results in electron transfer[23]. The inclusion of metal nanocatalysts to the reaction mixture may act as a possible intermediary between the MB dye and the BH_4^- ions. It may further be said that the reduced bond dissociation energy and increased the efficiency of electron transport between them[24]. In the presence of metal nanoparticles, the rate of degradation of MB by $NaBH_4$ was enhanced. In the catalytic reduction of an organic dye, synthesized colloidal metal nanoparticles produced from readily accessible leaf extract exhibited good results.

The Table 1 is compared data with earlier reported studies. The present study exhibit fast catalytic activity in dye degradation with Ag-NPs/Au-NPs/ Ag-Au /Au-Ag NPs synthesized using litchi leaf extract.

Conclusion

Litchi leaf extract was utilized as a reducing and stabilizing agent to create bimetallic (Ag-Au/Au –Ag NPs) nanoparticles in a simple, non-hazardous, economical, and environmentally friendly manner. UV-visible, DLS, zeta potential and TEM measurements of the produced nanoparticles indicated that the average size of the Ag-Au bimetallic nanoparticles was between 23 nm and bimetallic nanoparticles are quite stable. The bimetallic nanoparticles (Ag-Au) NPs are demonstrated to be more effective catalysts with increase in rate of MB dye degradation.

Acknowledgement

The authors acknowledge the support received in carrying out TEM characterizations from department of SAIF and CIL, Panjab University, Chandigarh.

References

1 Magnusson M H, Deppert K, Malm J O, Bovin J O & Samuelson L, *J Nanoparticle Res*, 1 (1999) 243.
2 Lansdown A B G, *Curr Probl Dermatol*, 33 (2006) 17.
3 Contado C, *Front Chem*, 3 (2015) 48.
4 Santhoshkumar J, Rajeshkumar S & Kumar V S, *Biochem Biophys Reports*, 11 (2017) 46.
5 Singh P, Pandit S, S Mokkapati V R S, Garg A, Ravikumar V & Mijakovic I, *Int J Mol Sci*, 19 (2018) 1979.
6 Velmurugan P, Cho M, Lee S M, Park J H, Lee K J, Myung H & Oh B T, *J Saudi Chem Soc*, 20 (2016) 313.
7 Mody V, Siwale R, Singh A & Mody H, *J Pharm Bioallied Sci*, 2 (2010) 282.
8 Borah R & Verbruggen S W, *J Phys Chem C*, 124 (2020) 12081.
9 Zaleska-Medynska A, Marchelek M, Diak M & E Grabowska, *Adv Colloid Interface Sci*, 229 (2016) 80.
10 Sharma V K, Yngard R A & Lin Y, *Adv Colloid Interface Sci*, 145 (2009) 83.
11 Santos N M, Gomes A S, Cavalcante D G S M, Santos L F, Teixeira S R, Cabrera F C & Job A E, *IET Nanobiotechnol*, 13 (2019) 307.
12 Kaur R, Avti P, Kumar V & Kumar R, *Nano Express*, 2 (2021) 020005.
13 Hada A M, Potara M, Suarasan S, Vulpoi A, Nagy-Simon T, Licarete E & Astilean S, *Nanotechnology*, 30 (2019) 315701.
14 El-Naggar M E, Shaheen T I, Fouda M M G & Hebeish A A, *Carbohydr Polym*, 136 (2016) 1128.

15 Alzahrani H A H, Buckingham M A, Wardley W P, Tilley R D, Ariotti N & Aldous L, *Chem Commun*, 56 (2020) 1263.
16 Manjari G, Saran S, Radhakrishanan S, Rameshkumar P, Pandikumar A & Devipriya S P, *J Environ Manage*, 262 (2020) 110282.
17 Mata R, Bhaskaran A & Sadras S R, *Particuology*, 24 (2016) 78.
18 Farzaneh F & Haghshenas S, *Mater Sci Appl*, 3 (2012) 697.
19 Zhang Z, Moghaddam L, Hara I M O & Doherty W O S, *Chem Eng J*, 178 (2011) 122.
20 Ho Y S & McKay G, *Process Biochem*, 34 (1999) 451.
21 Wei X, Li X, Feng Y & Yang S, *RSC Adv*, 8 (2018) 11764.
22 Azeez F, Al-Hetlani E, Arafa M, Abdelmonem Y, Nazeer A A, Amin M O & Madkour M, *Sci Rep*, 8 (2018) 7104.
23 Xu L, Wu X C & Zhu J J, *Nanotechnology*, 19 (2008) 305603.
24 Riaz S, Ikram M, Naz S, Shahzadi A, Nabgan W, Ul-Hamid A, Haider A, Haider J, & Al-Shanini A, *ACS Omega*, 8 (2023) 5808.
25 Ghosh S, Roy S, Naskar J & Kole R K, *Sci Rep*, 10 (2020) 277.
26 Bogireddy N K R, Hoskote A K K & Mandal B K, *J Mol Liq*, 211 (2015) 868.
27 Kumar I, Mondal M, Meyappan V & Sakthivel N, *Mater Res Bull*, 117 (2019) 18.
28 Rabeea M A, Owaid M N, Aziz A A, Jameel M S & Dheyab M A, *J Environ Chem Eng*, 8 (2020) 103841.
29 Wongyai K, Wintachai P, Maungchang R & Rattanakit P, *J Nanomater*, 2020 (2020) 1.
30 Nakkala J R, Bhagat E, Suchiang K & Sadras S R, *J Mater Sci Technol*, 31 (2015) 986.